ELSEVIER

Biochimica et Biophysica Acta 1283 (1996) 151–162

BBA Biochimica et Biophysica Acta

Phosphatidylethanol as a ^{13}C-NMR probe for reporting packing constraints in phospholipid membranes

Alexander V. Victorov *, Theodore F. Taraschi, Jan B. Hoek

Department of Pathology, Anatomy, and Cell Biology, Thomas Jefferson University Medical College, JAH Room 271, 1020 Locust Street, Philadelphia, PA 19107, USA

Received 5 February 1996; accepted 2 May 1996

Abstract

$^{13}CH_2$-ethyl labeled phosphatidylethanol (PEth), a rare naturally occurring anionic phospholipid, was used to probe the interleaflet packing density difference in small and large unilamellar phospholipid vesicles (SUVs and LUVs, respectively). The intrinsically tighter lipid packing in the inner leaflet of the SUVs resulted in the splitting of the CH_2-ethyl ^{13}C-resonance into two distinct components originating from PEth molecules residing in the inner and outer leaflets. The splitting of the ^{13}C-NMR signal from the PEth headgroup appears to be unique among naturally occurring phospholipids. We present data suggesting that the splitting of the PEth signal reports on transleaflet packing density difference modulated by unequal electrostatic interactions and structured water on the inner and outer surfaces of the SUV. The PEth resonance splitting was insensitive to pH changes over the range 5.3–8.6 and cannot be accounted for by differences in the pK_a of PEth in the inner and outer monolayers of the SUV. In ^{13}C-NMR spectra of LUVs, where packing constraints in both monolayers are approximately similar, only a single, narrow symmetrical CH_2-ethyl signal was observed, which was shifted downfield at higher PEth concentrations. The carbonyl and C_3-glycerol backbone PEth resonances were shifted upfield compared to those of phosphatidylcholine or phosphatidylglycerol, suggesting a more tightly packed/hydrophobic environment for these segments of the PEth molecule in the membrane. We conclude that the unique splitting of the PEth ^{13}C-resonance reported here can be used to characterize the lipid packing conditions in various membranes and to monitor the transbilayer distribution/movement of PEth.

Keywords: Phosphatidylethanol; NMR, ^{13}C-; Liposome; Packing constraint; Electrostatic force; Anionic phospholipid; Chaotropic anion; Phospholipid hydration

1. Introduction

In many biological membranes two monolayers of the same bilayer possess different packing densities due to an asymmetric distribution of certain membrane constituents, e.g., cholesterol, proteins and even phospholipid molecular species [1,2]. Unfortunately, this interesting membrane property has largely remained outside the scope of the capabilities of ^{13}C-NMR spectroscopy, one of the less invasive but probably most informative physico-chemical methods used to study model and biological membranes. As reported earlier [3–7], the chemical shift of the ^{13}C-resonances (compared with ^{1}H and ^{31}P) originating from the headgroups of major phospholipids is not sufficiently sensitive to detect the transbilayer differences in packing constraints.

Recently, we demonstrated [8] that phosphatidylethanol (PEth), an unusual naturally occurring anionic phospholipid [9–11], is an exception to this rule. Specifically, we showed that one can easily resolve two signals in the ^{13}C-NMR spectra from $^{13}CH_2$-ethyl labeled PEth molecules located in the inner and outer leaflets of small unilamellar vesicles (SUVs) without applying shift reagents. However, the origin of this splitting remains unknown. PEth possesses a small and relatively hydrophobic ethyl headgroup which can confer unusual membrane properties to this anionic phospholipid [12,13].

Here, we present data suggesting that the observed splitting of the $^{13}CH_2$-ethyl resonance reflects the difference in packing constraints between the two monolayers

Abbreviations: PC, phosphatidylcholine; PG, phosphatidylglycerol; PEth, phosphatidylethanol; SUVs, small unilamellar vesicles; LUVs, large unilamellar vesicles; NMR, nuclear magnetic resonance; TLC, thin-layer chromatography.

* Corresponding author. Fax: +1 (215) 9232218; e-mail: viktorol@jeflin.tju.edu.

PII S0005-2736(96)00096-X

which is due to differences in intrinsic curvature in the leaflets of the SUV membrane and which, in turn, results in different electrostatic interactions and structured water effects on the inner and outer surfaces of the SUV.

2. Materials and methods

Dioleoylphosphatidylcholine (PC) was purchased from Avanti Polar Lipids. Dioleoylphosphatidylethanol (PEth) was synthesized from PC via a transphosphatidylation reaction catalyzed by peanut phospholipase D (EC 3.1.4.4; Sigma) using [1-^{13}C]ethanol (99%) (Cambridge Isotope Laboratories) as described in detail elsewhere [8]. All other reagents were obtained from Sigma.

To prepare vesicles, PC and PEth were pre-mixed in chloroform, which was then evaporated under stream of nitrogen at 30°C; the obtained lipid films were kept overnight under deep vacuum (7 μm Hg) in a freeze dryer to remove any traces of chloroform. SUVs (40 mg/ml concentration of PC, 5 mM Na acetate (or 10 mM Tris-HCl) buffer containing 25% D_2O with or without 130 mM NaCl) were prepared by ultrasonic irradiation of a hand-shaken lipid dispersion (placed in ice water) to constant optical clarity (450 nm), using a MedSonic W-225 sonicator operating at 20 kHz (power setting of 4–5) with a 3.2 mm microtip (typically 6–9 five min cycles with 3 min on/2 min off). The SUVs obtained were purified from metal particles and any remaining multilamellar liposomes by high speed (43 000 × g, 20 min) centrifugation as described earlier [8]. In addition, some SUV preparations were subjected to a subsequent ultracentrifugation (106 000 × g, 60 min). However, this procedure resulted in no changes in the ^{13}C-NMR spectral parameters and, consequently, ultracentrifugation was not usually employed. The composition of purified SUVs corresponded to the initial PC/PEth ratio as demonstrated by TLC, which was used to analyze vesicles with high (5–43%) PEth concentrations. For low (0.5–2%) PEth levels, the PC/PEth ratio was determined by comparison of integral intensities of ^{13}C resonances, i.e., the OCH_2-choline (for PC) and CH_2-ethyl (for PEth), using 1% ^{13}C-enrichment for PC and 90% ^{13}C-enrichment for PEth (our NMR data). The presence of phospholipid degradation products (such as lyso-forms and peroxides) in the SUV samples was examined under all experimental conditions used, i.e., immediately after sonication and after low pH or high temperature incubations. In every case the lyso-PC and lyso-PEth content remained below 1% (TLC data); no significant formation of lipid peroxides was detected, as indicated by the constant peroxidation index A_{233}/A_{215} [14,15].

LUVs were prepared in the same buffer as SUVs by an extrusion procedure applying 27–29 passes through two stacked 100 nm pore polycarbonate filters in a LiposoFast extrusion apparatus (Avestin) as described earlier [8].

^{13}C-NMR broadband decoupled 90.6 MHz spectra were obtained on a Bruker AM 8.5T WB spectrometer in a 10 mm double resonance probe without sample spinning as described in detail earlier [8]. Briefly, unless otherwise stated, we used the following typical conditions: 45° flip

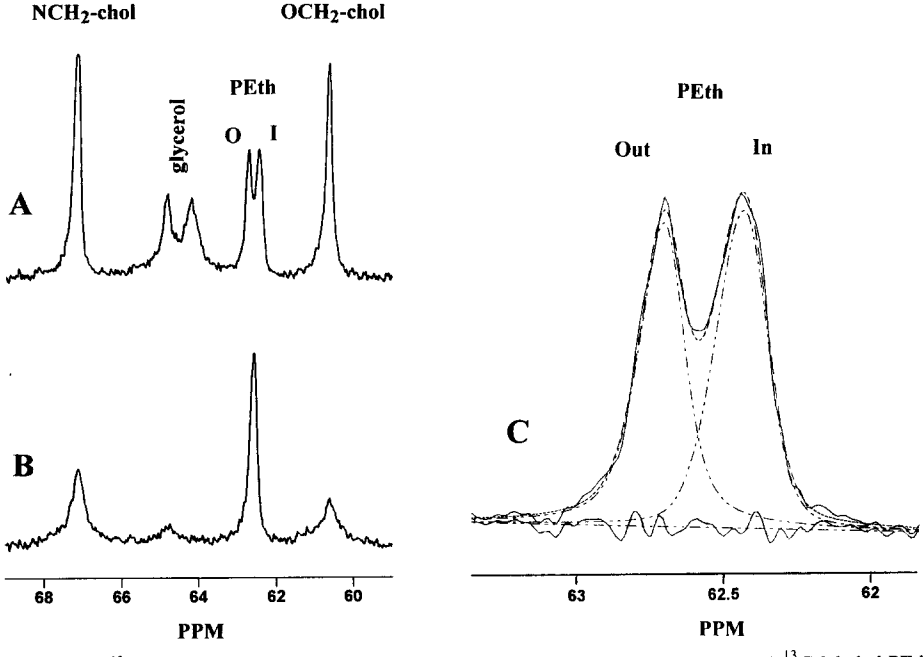

Fig. 1. The headgroup region of the ^{13}C-NMR spectra of SUVs (A) and LUVs (B) composed of 99% PC and 1% ^{13}C-labeled PEth (5 mM sodium acetate buffer pH 6.5, T = 296 K); (C) shows the expanded $^{13}CH_2$-ethyl peak region of the spectrum A, illustrating closely matching experimental (solid line) and simulated (dashed line) doublets, residual signal (solid line at the baseline) and separate outer and inner PEth peaks (dash-dotted lines) (for details for computer simulation see Section 2).

angle, 20.1 kHz broadband ^{1}H-decoupling power, 3.6 kHz broadband irradiation between acquisitions for NOE generation, 1.2 s pause between acquisitions, 20 kHz spectral window, 8 K data points zero-filled to 16 K and 1 Hz exponential filtering. Number of scans varied from 1500 to 6000. In addition, T_1 and NOE were measured for both the 'inner' and 'outer' PEth CH_2-ethyl signals for each sample and were found to show no significant differences [8]. Thus, the ratio of their integral intensities I_{in}/I_{out} can be used to characterize the transbilayer distribution of PEth. Chemical shifts were taken relative to the acyl CH_3-terminal signal (assigned to 15.05 ppm for PC vesicles [16]). All signal assignments in the spectra were made as described elsewhere [16,17].

To fully resolve the partially overlapping outer and inner PEth signals we used a combination of two methods. First, we applied externally the shift reagent Pr^{3+} at low concentrations of 0.2–0.3 mM, which substantially shifts the outer peak further downfield without affecting the transbilayer distribution of PEth. This enabled us to accurately determine the spectral parameters of the inner PEth signal, i.e., its integral intensity (measured relative to the acyl methyl peak) and its line-shape, line-width and chemical shift. Then, the integral intensity of the outer peak can be obtained by subtracting the inner peak intensity from the total (doublet) intensity. Subsequently, the spectral parameters obtained were used in a simulation procedure. For this, we used a Dell IBM Pentium/133 computer and NMR version of the GRAMS/386 software assuming a mixed (gaussian + lorentzian) peak shape for both the inner and outer PEth signals. The simulated signals closely matched those in experimental spectra with respect to relative intensity and chemical shift. The simulated spectra are presented as an illustration of the fit only in Fig. 1C. However, quantitative data obtained from these computations and from the shift reagent approach were used in every experiment where the signal intensities were compared.

3. Results

3.1. Splitting of the $^{13}CH_2$-ethyl PEth signal into the inner and outer components is observed for SUVs but not for LUVs

Fig. 1A shows the headgroup region of the ^{13}C-NMR spectrum of SUVs composed of PC-1% ^{13}C-labeled PEth. The CH_2-ethyl signal from the PEth headgroup is registered in a chemical shift range of 62.8–62.4 ppm, between other signals from the PC headgroup and the glycerol backbone. The CH_2-ethyl peak consists of two components: the peak shifted downfield originates from PEth molecules localized in the outer leaflet, while the upfield peak derives from PEth molecules residing in the inner leaflet. The assignments of the two signals were made with the aid of shift (Pr^{3+}) and broadening (Mn^{2+}) reagents in our previous work [8]. For low (1%) PEth concentrations (Fig. 1A) the intensities of the outer and inner peaks were roughly the same. Since the inner surface is only about one half of the external surface area in SUVs, this intensity ratio indicates a strong preference of PEth for the inner leaflet of the SUV. For higher (16.7–43%) concentrations of PEth, the outer PEth signal was approximately twice as large as the inner one (Fig. 2A), suggesting a more symmetric transmembrane distribution of PEth in the SUV bilayer.

Since the lipid packing density in the inner and outer leaflets of the highly curved SUV membrane is intrinsically unequal (i.e., the inner monolayer is packed significantly tighter) [4,18,19], we suggested that this splitting, $\Delta\delta = \delta_{out} - \delta_{in}$, is due primarily to different packing constraints in two monolayers. This interpretation is supported by the observation that an unsplit and rather narrow CH_2-ethyl PEth signal (e.g., compare with CH_2-choline signals) was obtained from 100 nm LUVs (Fig. 1B), with a chemical shift intermediate between the outer and inner PEth resonances in 27 nm SUVs. The LUV membrane is significantly less curved than that of SUVs and, hence, packing conditions for phospholipid molecules on the inner and

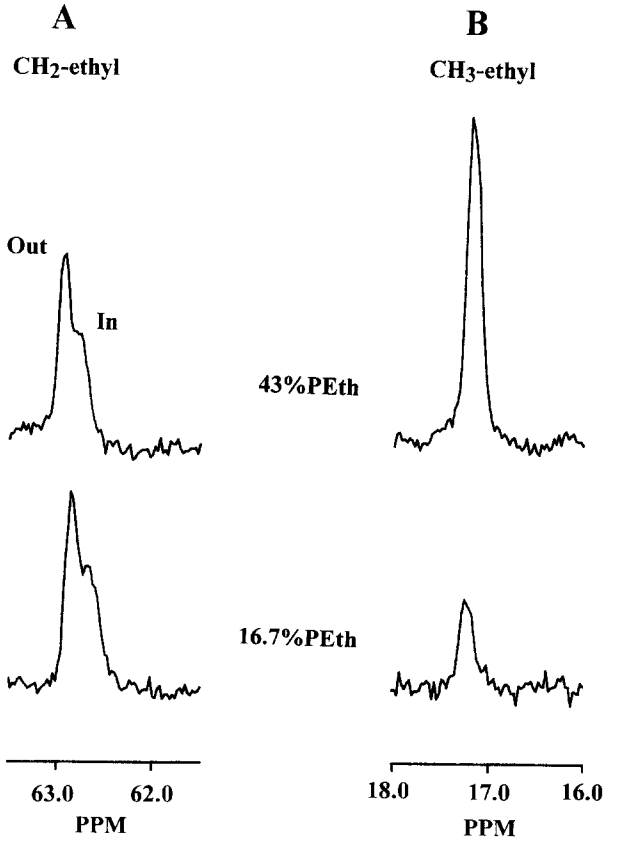

Fig. 2. ^{13}C-NMR spectra regions showing the PEth headgroup signals from SUVs with high concentrations of unlabeled PEth: (A) the CH_2-ethyl signal region, the bottom sample also contains 1% $^{13}CH_2$-ethyl labeled PEth; (B) the CH_3-ethyl signal region; (5 mM K acetate buffer with 100 mM KCl, pH 7.2, T = 295 K).

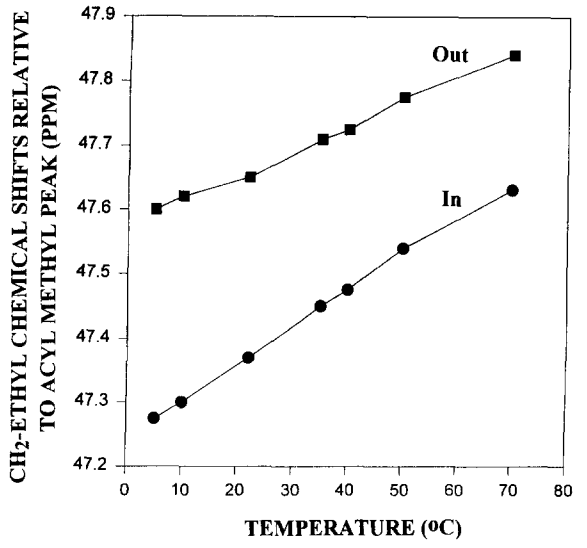

Fig. 3. Temperature dependence of the splitting between the inner and outer PEth signals in PC-1% PEth SUVs (5 mM Na acetate buffer, pH 6.6).

outer surfaces are essentially the same [20], as manifested by the lack of splitting of the CH_2-ethyl PEth signal.

The second signal of the PEth headgroup (from an unlabeled CH_3-moiety) is observed around 17.17 ppm (Fig. 2B). This signal is narrower than CH_2-ethyl peak and only slightly asymmetric (though for some samples a minute splitting was observed, presumably between the inner and outer components). This suggests that the CH_3-ethyl group experiences both a relatively high motional freedom and similar environments in both leaflets.

The expanded region of the experimentally obtained PEth $^{13}CH_2$-ethyl doublet (spectrum 1A) together with the simulated curve, residual signal and separate outer and inner peaks are shown in Fig. 1C. The chemical shifts and integral intensity ratio I_{in}/I_{out} (1.07) for the simulated peaks closely resemble those for the experimental signals. Both the inner and outer signals have approximately the same line-width (19–21 Hz), though the line-shape of the outer PEth peak tends to be more lorentzian than that of the inner peak (see Section 2).

3.2. Increasing temperature decreases the PEth signal splitting

The role of lipid packing density in determining the degree of splitting of the PEth signal into the inner and outer components was further assessed by studying the effect of temperature, since this parameter can alter the difference in lipid packing density inside and outside the SUV [4,7]. As shown in Fig. 3, increasing the temperature substantially diminished the splitting between the outer and inner PEth signals, mainly at the expense of the greater downfield shift of the inner signal, indicating that the packing constraints for PEth in the inner leaflet at elevated temperature approach those on the outer surface of the SUV. A similar effect was recently observed for the inside/outside splitting of the PC *N*-methyl proton resonance [7].

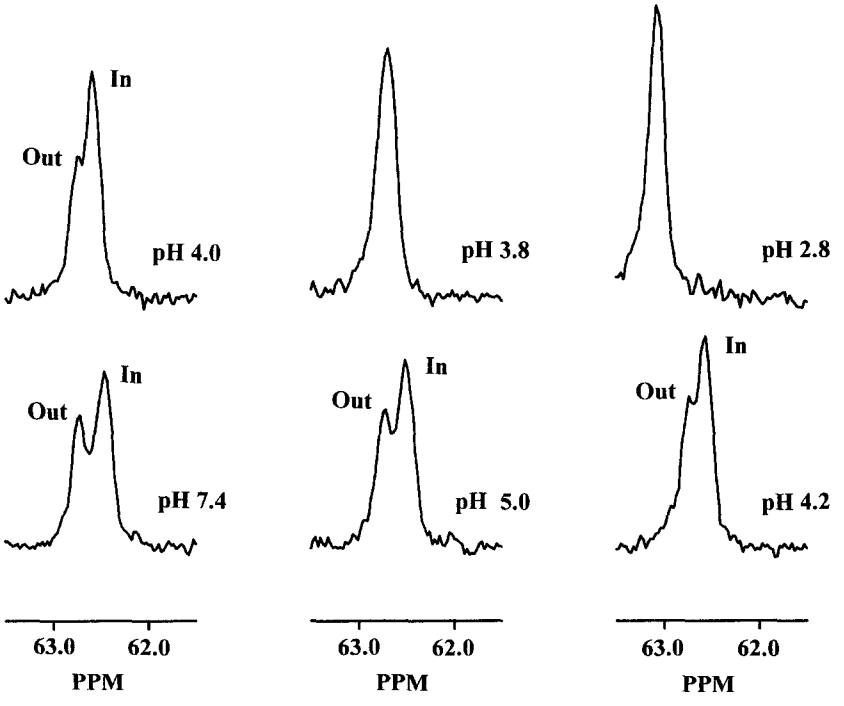

Fig. 4. Influence of pH on the splitting and inside/outside ratio for the inner and outer CH_2-ethyl signals (PC-2%PEth SUVs, 5 mM Na acetate buffer with 100 mM KCl, $T = 295$ K); I_{in}/I_{out} were: 1.35 (pH 7.4), 1.39 (pH 5.0), 1.44 (pH 4.2), 1.83 (pH 4.08) and 3.6 (pH 3.8).

3.3. PEth signal splitting is not due to different pK_a inside and outside the SUV

Differences in packing density in the outer and inner monolayers of the SUV could be reflected in different apparent pK_a values of PEth molecules residing on two surfaces. This effect would be manifest in a pH dependence of the PEth peak splitting at pH values in the vicinity of the pK_a.

We measured the pH dependence of the chemical shift of both the inner and outer PEth signals in PC-2%PEth SUVs. As seen from Figs. 4 and 5, for $5.3 < pH < 7.4$ there were no detectable changes in either chemical shifts of both the inner and outer PEth signals (and, hence, in $\Delta\delta$), or in the inner/outer signal intensity ratio ($I_{in}/I_{out} = 1.35$). However, at approximately $4.4–4.6 < pH < 5.2$ the inner signal started moving downfield without noticeable changes in its intensity (at pH 5.0 $I_{in}/I_{out} = 1.39$), with the outer signal unchanged. The main cause for a downfield shift of the CH_2-ethyl signal from the inner PEth is its partial protonation in this pH region, while the outer PEth remained fully negatively charged. Had some of the outer PEth molecules been protonated, they would have rapidly moved to the inner surface which, due to a tighter packing, favors the accommodation of the uncharged phospholipids with a small headgroup. This, in turn, would have increased the intensity of the inner signal at the expense of the outer one. This was not observed. This indicates that the pK_a of PEth on the inner surface is higher than that on the outside (by approx. 0.6–0.8 pH units). However, the situation was changed at $pH < 4.4–4.6$ when the continued downfield shift of the inner signal was accompanied by an increase in its intensity while the intensity of the outer peak decreased, suggesting that some outer PEth molecules became protonated and migrated to the inside (at pH 4.08

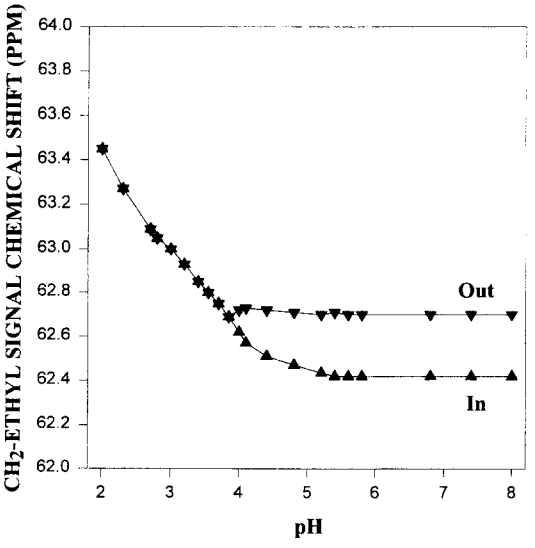

Fig. 5. pH titration of SUVs composed of PC-2%PEth in 5 mM Na acetate buffer with 100 mM KCl ($T = 295$ K).

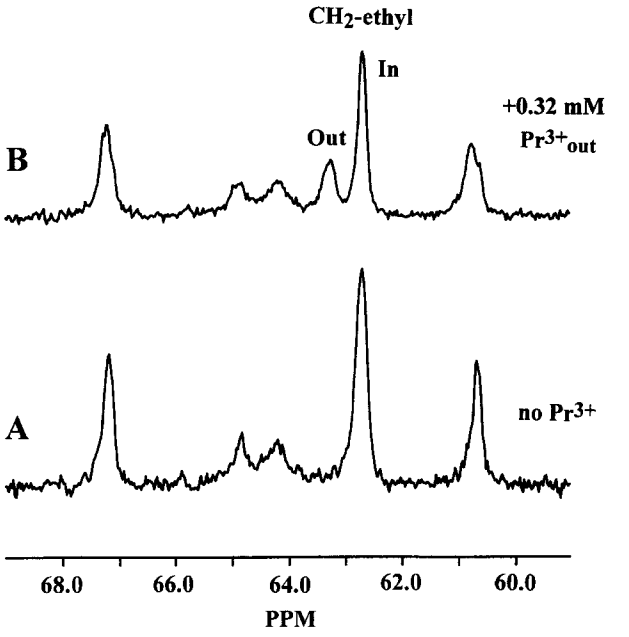

Fig. 6. Addition of 0.32 mM Pr^{3+} to PC-2%PEth SUVs at pH 3.8 splits the merged CH_2-ethyl signal into the inner and outer components ($T = 295$ K, 100 mM KCl): (A) no Pr added; (B) after addition of 0.32 mM Pr^{3+} to the outer medium.

$I_{in}/I_{out} = 1.83$). At pH 3.8–3.9 (and below) the two PEth peaks merged (Figs. 4 and 5). The coalescence of two signals was not due to fast exchange of PEth molecules between two surfaces as evidenced by the fact that the inner and outer components could be resolved by addition of a shift reagent (0.32 mM Pr^{3+}) to the outer medium (Fig. 6). Also, the spectrum 6B clearly demonstrates that at pH 3.8 a substantial portion of the outer PEth flipped to the inner leaflet ($I_{in}/I_{out} = 3.6$). Judging by an apparent inflection point of the titration curve (about 3.7–3.9) and the onset of changes in the chemical shifts and intensities of the inner and outer PEth peaks, we tentatively estimate the pK_a as 3.7–3.9 and 3.0–3.2 for the inner and outer PEth, respectively.

It is important to note that the titration curve for the CH_2-ethyl peak for the PC-2%PEth vesicles does not level off until the pH approaches zero [8], most likely due to a substantial downfield shift caused by structural changes in the vesicles owing to protonation of PC for which a pK_a close to 1 was reported [21]. Changes in the chemical shift of the PEth signal observed at pH 3–5 are minor compared to the changes occurring at $pH < 2–3$ and, hence, can be easily overlooked. Thus, our earlier estimate of a pK_a for PEth in the PC-2%PEth LUVs was probably underestimated [8].

3.4. PEth signal splitting diminishes as the concentration of negatively charged phospholipids increases

The presence in the PC bilayer of PEth, as a negatively charged species, can in principle change the pattern of the

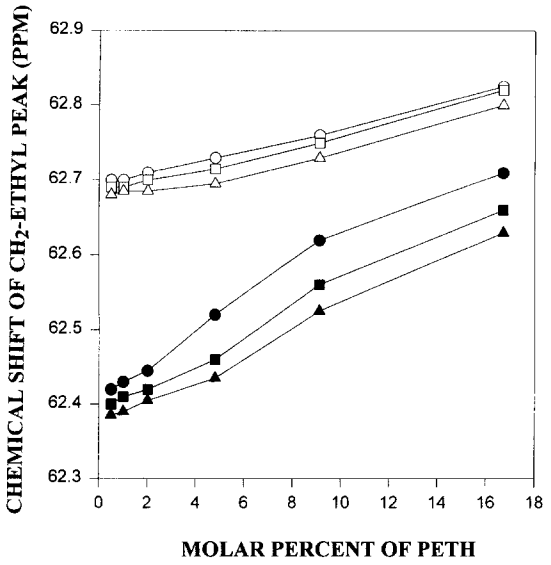

Fig. 7. Dependence of chemical shifts of the inner (filled symbols) and outer (open symbols) PEth CH_2-ethyl signals on concentration of PEth in PC-PEth SUVs and ionic strength (5 mM K acetate buffer, pH 6.7, $T = 295$ K): no KCl (circles); 100 mM KCl (squares); 500 mM KCl (triangles); (the relative error was ± 0.005 ppm).

phospholipid packing in both monolayers as a consequence of PC–PEth and PEth–PEth electrostatic interactions. Obviously, these interactions would depend on the concentration of PEth. This, in turn, would be expected to influence the splitting of the PEth resonance. Indeed, at lower concentrations of PEth (0.5–2%) the splitting $\Delta\delta$ between PEth peaks was larger than at high PEth levels (Fig. 7, Table 1). The chemical shifts of both the inner and outer PEth signals were concentration dependent and increased with increasing PEth concentrations. However, the greater downfield shift of the inner peak caused a reduction in the splitting. This effect of PEth was partly shielded by high concentrations of KCl. In the absence of KCl the inner and outer PEth signals were poorly resolved already at 9.1% PEth, whereas in the presence of 100 mM or 500 mM KCl two separate PEth signals could be observed even at 16.7% PEth. The incorporation of 15.7% of another anionic phospholipid, namely PG (while retaining 1% ^{13}C-labeled Peth), in the SUVs resulted in a spectrum that closely resembled that of Fig. 2A, i.e., the addition of PG to SUVs containing 1% PEth also decreased the PEth splitting, analogous to the curves of Fig. 7: both signals were shifted downfield, with the inner signal approaching the outer one (see also Fig. 8C top). By contrast, no splitting was observed for the headgroup ^{13}C-signals from PG. These findings indicate that the PEth peak splitting is reduced in the presence of negative charges on the membrane, implying a role for electrostatic interactions.

3.5. Chaotropic anions increase the PEth signal splitting

To further examine the role of membrane surface charge density in the splitting of the PEth resonance and test the possible modulation imposed on such splitting by structured water effects, we prepared SUVs containing either 1% PEth, or 16.7% PEth, or 15.7% PG-1% PEth, in the presence of either 130 mM NaCl or 130 mM $NaClO_4$ (Fig. 8). Chloride anions do not adsorb on the membrane surface, while chaotropic perchlorate anions, owing to their ability to disrupt the structured water layers on the surface of the membrane, bind strongly to the PC membrane, thus providing it with an excess negative surface charge [7,22,23]. As shown in Fig. 8, in the presence of ClO_4^- the splitting of the PEth peak did not decrease. By contrast, perchlorate caused $\Delta\delta$ to be somewhat (20–35%) augmented, compared to the signal from vesicles prepared in NaCl, mainly due to a small downfield shift of the outer peak (Fig. 8). This effect was more pronounced for lower concentrations of PEth and must probably be attributed to a lower negative surface charge density of the membrane and, hence, an increased adsorption of anions compared to the inner surface. It is noteworthy that the strong binding of ClO_4^- on the membrane also shifted the transbilayer distribution of PEth in favor of the outer surface, which is particularly noticeable for 1% PEth concentration (Fig. 8A) compared to 16.7% PEth (Fig. 8B). A similar, but less pronounced effect was obtained with a less potent chaotropic anion, SCN^- (spectra not shown). When the major portion of PEth was replaced with another anionic phospholipid, PG, the perchlorate-induced increase in $\Delta\delta$ was observed as well (Fig. 8C), comparable to that of PEth alone (Fig. 8B), again largely at the expense of the low-field shift of the outer PEth signal.

When chaotropic anions (perchlorate) were applied to PC-PEth LUVs, similar data were obtained (Fig. 9, Table 2). Specifically, in the presence of perchlorate (130 mM) on both sides of the membrane the total CH_2-ethyl signal

Table 1
PEth concentration dependence of $\Delta\delta$, splitting (ppm) between the outer and inner PEth signals for PC-PEth SUVs (5 mM Na acetate buffer, pH 6.5, $T = 295$ K)

	$\Delta\delta$ at a PEth concentration of							
	0.1%	0.25%	0.5%	1.0%	2.0%	4.8%	9.1%	16.7%
No KCl	0.30	0.29	0.28	0.27	0.265	0.21	0.14	0.12
100 mM KCl	0.30	0.29	0.29	0.28	0.28	0.255	0.195	0.16
500 mM KCl	0.30	0.30	0.30	0.295	0.28	0.26	0.205	0.17

The relative error was ± 0.005 ppm.

of PEth was shifted downfield, this effect being reduced at higher concentrations of PEth (though the increased concentration of PEth itself caused an analogous shift). The magnitude of this perchlorate-induced shift of the PEth signal in LUVs was close to that of the outer PEth signal in the spectra of PC-PEth SUVs (Table 2).

3.6. Carbonyl and glycerol backbone signals report that PEth is positioned in the membrane in a more tightly packed / hydrophobic environment than PC

The relatively hydrophobic ethyl headgroup of PEth can cause a different orientation of the whole molecule in the bilayer compared to that of PC or other natural phospholipids. Analysis of the chemical shifts of the other signals from PEth segments positioned in the interface, i.e., carbonyl and glycerol backbone ones, can provide important information on this account. First, we compared the chemical shifts of the carbonyl resonances of PC, PG and PEth in the spectra of the SUVs composed of either PC, or PC-43%PG, or PC-43%PEth mixture (Fig. 10). In full accordance with earlier data [16,24], two well resolved carbonyl peaks were observed in the ^{13}C-NMR spectra of the PC vesicles (Fig. 10A): a larger downfield-shifted resonance from the molecules located in the outer leaflet and a smaller resonance from the inner leaflet molecules. Both peaks are, in turn, split into two components attributed to α- and β-carbonyl groups of the same molecule [24]. However, this much smaller splitting is frequently poorly resolved and was difficult to observe under our experimental conditions. Analoguous carbonyl splitting (doublet) was found for SUVs prepared from PC-43%PG mixture (Fig. 10B), demonstrating identical packing environments for both PC and PG. However, in the spectra of SUVs with a high concentration (43%) of PEth (Fig. 10C) two PEth carbonyl peaks, distinct from those of PC, were registered; both were shifted upfield relative to the corresponding PC resonances and partially superimposed on the two PC carbonyl peaks. The outer PEth carbonyl peak was approximately twice as large than the inner peak (similar to PC) and was positioned immediately over the inner PC carbonyl signal. The upfield shift of both the outer and inner PEth carbonyl signals clearly indicates that PEth is in a more tightly packed/hydrophobic environment, compared to either PC or PG, on both surfaces of the SUV. Because of the partial overlapping of the PEth and PC carbonyl signals, the difference in packing conditions of PEth between the two leaflets could not be accurately measured, though judging by the magnitude of the PEth inside/outside carbonyl splitting, it was not markedly different from that of PC. It is noteworthy that neither PEth nor PG, even at high 43% concentrations, changed the packing of PC, of which both carbonyl peaks remained unaffected in all samples (Fig. 10).

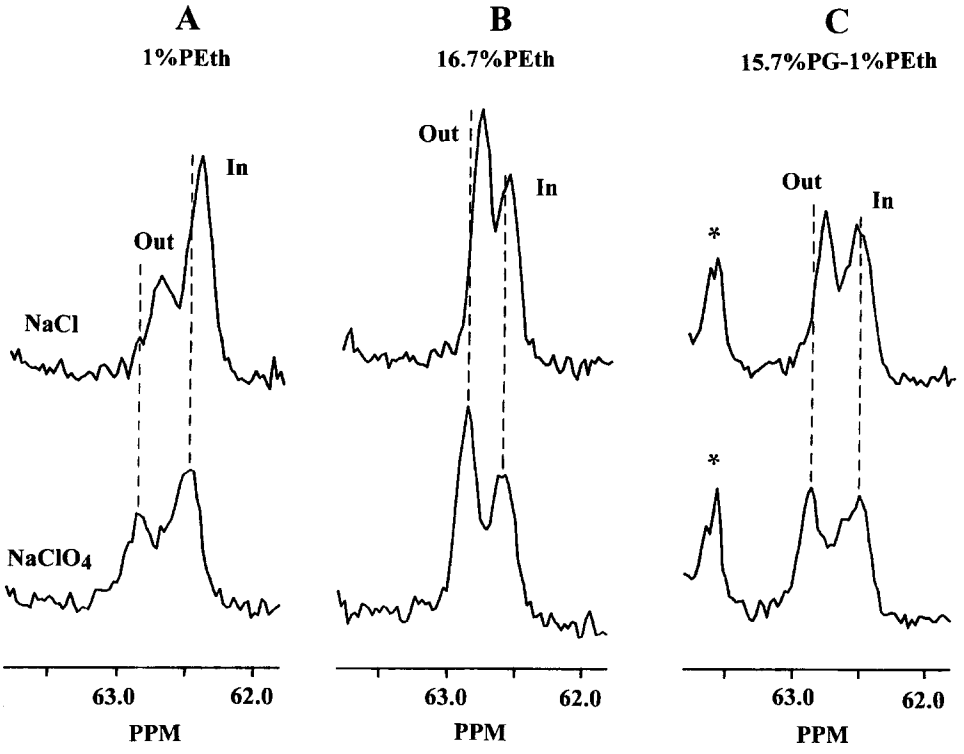

Fig. 8. Effect of 130 mM $NaClO_4$ (bottom panel) and 130 mM NaCl (top panel) present inside and outside PC-PEth SUVs (5 mM Na acetate buffer pH 6.4, $T = 295$ K) on the splitting between the inner and outer PEth signals, Δδ: (A) 1% PEth; (B) 16.7% PEth; (C) 15.7% PG-1% PEth (1% ^{13}C-labeled PEth was used in each sample); asterisk denotes a signal from the PG headgroup.

Since negatively charged phospholipids did not influence the carbonyl splitting of PC, we applied chaotropic perchlorate anions to these vesicles to examine the structured water effects on this splitting. As shown in Fig. 11 (bottom panel) ClO_4^- induced a downfield shift, relative to Cl^- (Fig. 11, top panel), mainly of the outer PC carbonyl peak to approximately the same extent for all samples, irrespective of the presence of rather high concentrations of PEth or PG.

Further analysis of the spectra of SUVs comprising PC-43%PEth revealed an analoguous unusual upfield shift for another PEth resonance, namely, for the C_3-glycerol peak positioned in close vicinity to the headgroup (Fig. 12C), compared to PC (Fig. 12A) or PC-PG vesicles (Fig. 12B). Relatively poor resolution and low signal/noise ratio of this resonance did not allow any measurements of its possible splitting. Upon acidification (at pH < 4.5, see Section 3.3), the C_3-glycerol PEth signal moved downfield and coalesced with the C_3-glycerol peak from PC (not shown). The most likely explanation for this effect of PEth would be an unusual conformation/orientation (relative to PC) for this segment of the glycerol backbone, or its location in a more tightly packed area. The other two PEth

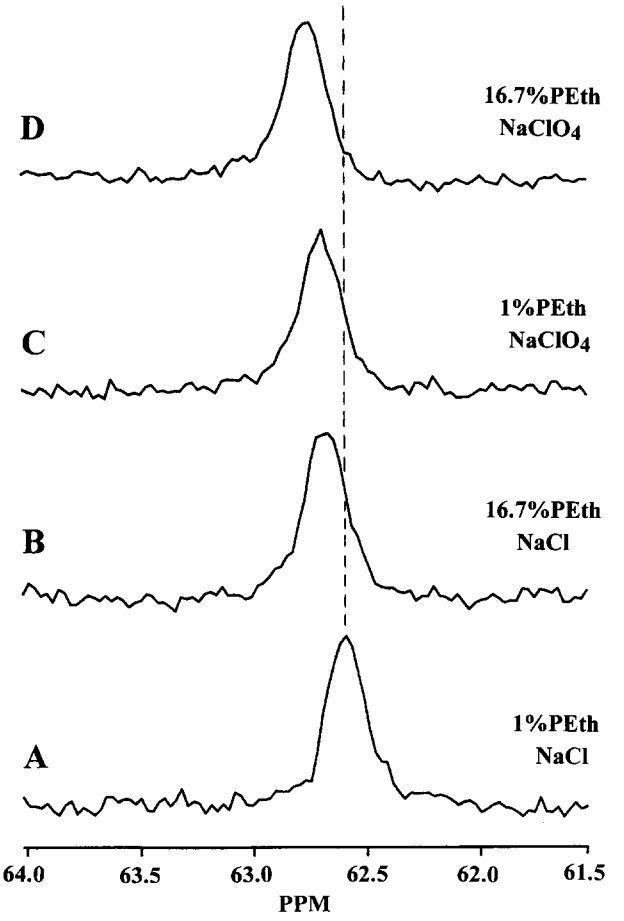

Fig. 9. PEth signal region of ^{13}C-NMR spectra of phosphatidylcholine LUVs containing different amounts of anionic phospholipids (1% ^{13}C-labeled PEth was used in each sample): (A) 1%PEth, 130 mM NaCl; (B) 16.7%PEth, 130 mM NaCl; (C) 1%PEth, 130 mM $NaClO_4$; (D) 16.7%PEth, 130 mM $NaClO_4$ (5 mM Na acetate buffer, pH 6.8, $T = 295$ K).

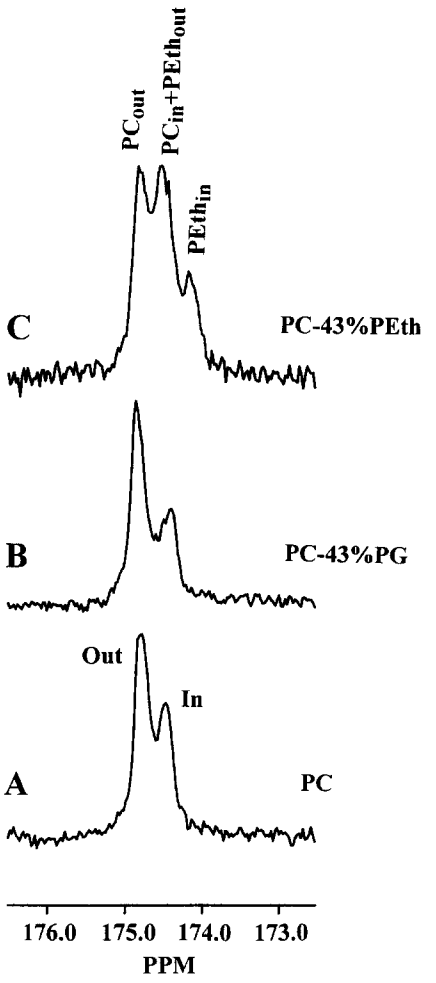

Fig. 10. Carbonyl ^{13}C-signals in the spectra of SUVs prepared from PC (A), PC-43%PG (B) or PC-43%PEth (C). To obtain the undistorted integral intensities for carbonyl signals, the interpulse delay was increased to 4 s (see Section 2); 150 mM NaCl and 10 mM Tris-HCl buffer, pH 7.2 were used; $T = 296$K.

Table 2
Perchlorate-induced downfield shift, $\Delta\delta_{anion}$, of the CH_2-ethyl signal in SUVs and LUVs containing low and high amounts of PEth

Vesicles	$\Delta\delta_{anion} = \delta_{ClO4} - \delta_{Cl}$ (ppm)			
	1% PEth		16.7% PEth	
	$(\Delta\delta_{anion})_{in}$	$(\Delta\delta_{anion})_{out}$	$(\Delta\delta_{anion})_{in}$	$(\Delta\delta_{anion})_{out}$
SUV	0.050 ± 0.005	0.144 ± 0.015	0.001 ± 0.005	$0.075 + 0.008$
	$(\Delta\delta_{anion})_{total}$			
LUV	0.112 ± 0.014		0.083 ± 0.008	

130 mM NaCl or 130 mM $NaClO_4$ were present on both sides of the membrane (5 mM Na acetate buffer pH 6.7, $T = 296$ K).

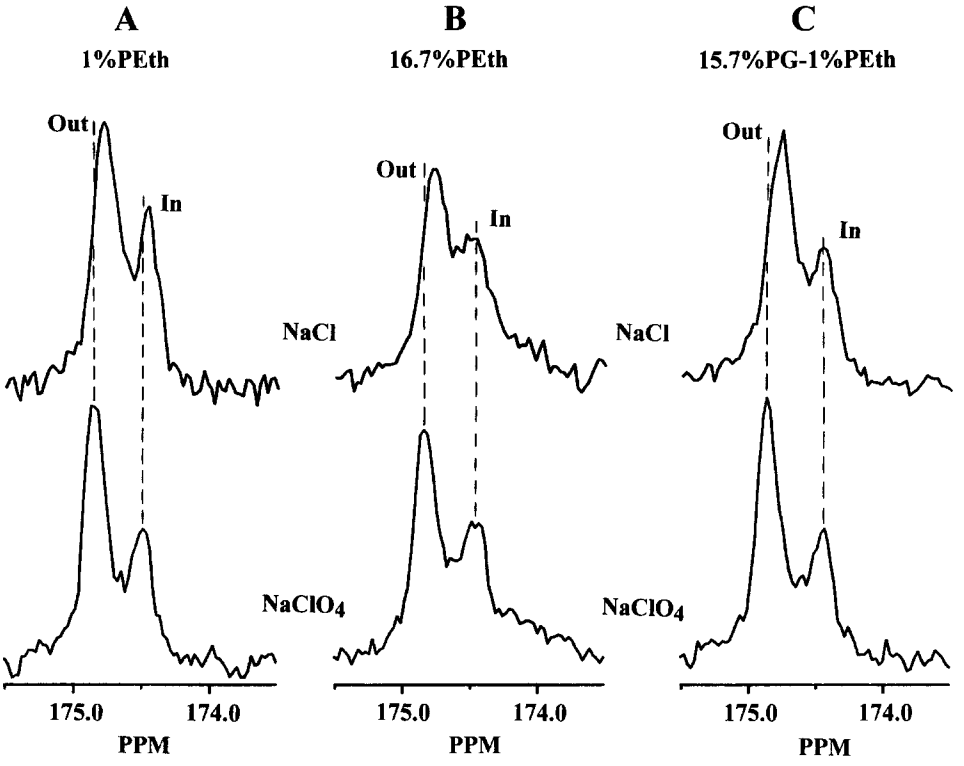

Fig. 11. Effect of 130 mM $NaClO_4$ (bottom panel) and 130 mM NaCl (top panel) on the PC carbonyl ^{13}C-signals for SUVs composed of: (A) PC-1%PEth; (B) PC-16.7%PEth and (C) PC-15.7%PG-1%PEth (5 mM acetate buffer, pH 6.4, $T = 295$ K); 1% ^{13}C-labeled PEth was used in each sample.

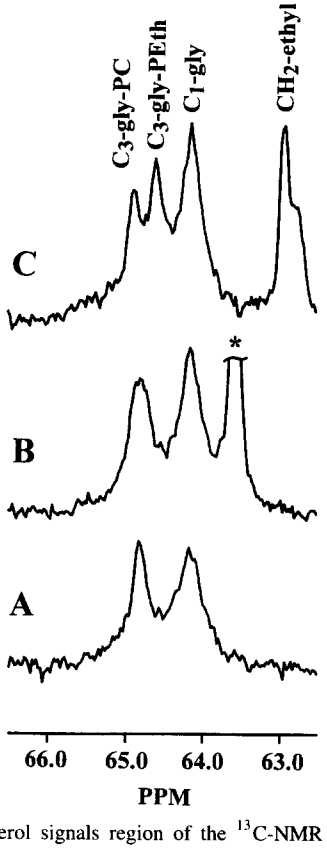

Fig. 12. 1,3-Glycerol signals region of the ^{13}C-NMR spectra of SUVs composed of either PC (A), PC-43%PG (B) or PC-43%PEth (C). Other experimental conditions as in Fig. 10. Asterisk denotes a signal from the C_3-PG headgroup.

glycerol peaks, i.e., from C_1- and C_2-carbons, were significantly broader and fully merged with the corresponding glycerol peaks from PC. Although an accurate estimate of possible small upfield shifts for these signals obviously could not be made (or any splitting detected), the whole envelopes (PC + PEth) representing the C_1- and C_2-glycerol resonances seemed to be also slightly shifted upfield compared to PC resonances in the absence of PEth. It is noteworthy that none of these changes in chemical shifts of the carbonyl or C_3-glycerol backbone signals were detected when PG was used instead of PEth, i.e., for SUVs prepared from the PC-43%PG mixture (Fig. 12B).

4. Discussion

4.1. The transleaflet difference in lipid packing constraints is the primary cause of the PEth resonance splitting in the SUV

A remarkable property of PEth incorporated into PC bilayers, which has been studied here, is the splitting of the CH_2-ethyl signal into the 'inner' and 'outer' components which permits the discrimination of the two leaflets of the SUV. For PC headgroup ^{1}H- and ^{31}P-NMR resonances an analoguous splitting for SUVs was documented long ago [3–7], but such an effect was not previously reported for ^{13}C-NMR signals (except for the splitting of the carbonyl

signals [16,24]). There is general agreement that the main cause of these splittings is the difference in lipid packing requirements between the outer and inner leaflets of the SUV [3–7]. As was demonstrated for choline *N*-methyl ^{1}H-resonances [5], when the vesicle size increases, the split between the inner and outer components diminishes. The same argument applies to the $^{13}CH_2$-ethyl signal where the splitting disappeared in the ^{13}C-NMR spectra of LUVs. In addition, the temperature dependence of the PEth peak splitting (Fig. 3) is analoguous to that found for the PC headgroup ^{1}H-splitting reported earlier [7], i.e., at higher temperature splitting was reduced, presumably because the transleaflet difference in packing constraints was decreased

The different packing conditions in the inner and outer leaflets of the SUV can cause the observed splitting of the CH_2-ethyl ^{13}C-resonance by several (not entirely independent) mechanisms, some of which would apply exclusively to PEth having a negative charge and an unusual hydrophobic headgroup. Specifically, the following effects may be different in two monolayers for PEth: electrostatic interactions, structured water, hydrophobicity of the environment and molecular conformation/orientation.

4.2. Electrostatic PC–PEth interaction

The shorter distance between the positively charged *N*-methyl group of PC and negatively charged phosphate group of PEth in the inner monolayer is expected to result in increased electrostatic interaction on this surface. Earlier, analyzing the splitting of PC headgroup resonances in SUVs, Hutton et al. [25] suggested that the tighter headgroup packing on the inside of the vesicles would result in stronger intermolecular *N*-methyl–phosphate interactions which, in turn, would induce upfield shifts of the ^{1}H and ^{31}P resonances from the inner molecules relatively to those in the outer monolayer. The observed splitting of the $^{13}CH_2$-ethyl signal of PEth in SUVs can be of the same origin. As the concentration of PEth in the membrane increases, the bilayer would expand somewhat electrostatically [26], thus increasing intermolecular distances and, hence, weakening PEth–PC electrostatic interactions. Consequently, both the outer and inner PEth signals move downfield, but the effect is more pronounced for the inner surface (Fig. 7), as a result of which splitting diminishes. An identical reduction in the PEth peak splitting was observed when another anionic phospholipid, PG, was used to increase the membrane surface charge at a constant low (1%) PEth level, thus excluding any electrostatic effects specific to PEth. In this context, it is noteworthy that the parallel orientation of the PC choline moiety on the membrane surface required for such interactions [25] is probably the same inside and outside the vesicles, despite the tighter packing in the inner leaflet. This suggestion is based on findings by Hauser et al. [27] who demonstrated that geometrical requirements imply that the minimal area per phospholipid molecule for parallel orientation of the PC headgroup should be 47–54 Å^2. This value is lower than published estimates of the PC molecular area in the membrane, e.g., 62 Å^2 [28] or 68 Å^2 [4], the actual area being larger probably due to dynamic and hydration phenomena.

4.3. Structured water effects as probed with chaotropic anions

Chaotropic anions used in this work (SCN^- and ClO_4^-) are known to adsorb strongly onto the PC membrane surface, thus charging it negatively [7,22,23]. The degree of adsorption correlates with the ability of a given anion to disrupt the structured water layers on the membrane surface. Earlier, a downfield shift of the PC proton resonance induced by chaotropic anions due to changes in the structured water shell was reported by Jendrasiak et al. [7]. According to the data obtained here for the LUV membrane (Fig. 9), which has a greatly reduced curvature, both the anionic phospholipids and chaotropic anions induce a downfield shift of the CH_2-ethyl signal. Thus, we can suggest that both effects produced by chaotropic anions, i.e., attachment to the membrane surface of a negative charge and perturbations in the hydration shell, would shift the PEth signal in the same downfield direction. Moreover, these two effects are interrelated and difficult to differentiate: the greater water structure breakage, the stronger anion adsorption.

One way to distinguish the structured water effects from those due to the negative charge, would be to apply chaotropic anions to a membrane already highly charged, e.g., one containing high concentrations of the anionic phospholipid. In this case, adsorption of anions should not further increase dramatically the membrane surface charge density and, hence, any effects observed should be mainly due to changes in structured water. However, this is complicated by the possibility that anion binding might be noticeably reduced if the membrane contains higher concentrations of anionic phospholipids. The fact that perchlorate anions do adsorb on such negatively charged surfaces was demonstrated by the additional downfield shift of the PEth resonance for LUVs in Fig. 9 (compare spectra B and D). We suggest that this perchlorate-induced downfield shift was most likely attributed to changes in structured water.

For the highly curved SUV membrane with asymmetric distribution of the anionic phospholipids, the situation is more complex: the surface charge density, structured water shells and phospholipid packing pattern probably are different on the inside and outside. The question arises, therefore, to what extent this contributes to the splitting of the PEth signal. SUVs containing high concentrations of PEth (17–43%) have a nearly symmetric transleaflet distribution of PEth (see Fig. 2A). Thus, the surface charge density is rather high and similar in magnitude in both surfaces. The application of perchlorate to both the inner

and outer surfaces should greatly reduce or eliminate any transleaflet differences in effects of structured water. It should be emphasized that the total inside-outside difference in hydration, characteristic for highly curved membranes, would largely be preserved under these conditions. Had the PEth splitting been mainly due to these differences, it would have been dramatically decreased. However, in this case the splitting did not diminish, but actually was increased (by 20–25%), largely because of the greater downfield shift of the outer signal (Fig. 8). This observation indicates that the existing difference in structured water between the inner and outer surfaces of the SUV actually decreases the splitting of the PEth signal, the major source of which must be unequal lipid packing density between monolayers. Our data suggest that structured water effects are more noticeable on the outer surface of the SUV, which probably reflects the looser packing and more hydrated state of phospholipids in the outer monolayer.

By contrast, high concentrations of anionic phospholipids (PEth itself or PG) in the SUV caused a greater downfield shift of the inner signal which resulted in a decrease of the splitting of the PEth signal. The most likely explanation for this effect would be an electrostatic expansion of the bilayer [26] diminishing the transleaflet difference in the area per phospholipid molecule. Not unexpectedly, membrane-anchored charged molecules, such as PEth and PG, appear to be more effective in decreasing lipid packing density compared with the surface adsorbed anions.

4.4. The orientation of PEth in the membrane is different compared to other natural phospholipids

The splitting of the CH_2-ethyl PEth headgroup signal differs in two important aspects from those reported earlier for PC [4–6]: first, splitting of the headgroup ^{13}C-resonance was observed, which was never documented for other phospholipid headgroup carbon signals; second, this splitting was found for the signal from the CH_2-ethyl group positioned close to the negatively charged phosphate moiety of PEth, but much less for the CH_3-ethyl group. The higher sensitivity of the $^{13}CH_2$-ethyl signal of PEth (in comparison with PC) to the membrane curvature indicates that this headgroup has a significantly different conformation and/or orientation on the inside and outside of the vesicle, whereas the orientation of PC headgroup is always approximately parallel. We suggest that on the inner, more tightly packed surface, the CH_2-ethyl group is bent inward, but on the outer surface (or in the LUV), under looser packing conditions, this group is shifted somewhat more towards the aqueous boundary of the interface; the CH_3-ethyl group remains oriented inward in both cases (also see [29]). These different conformations of the PEth headgroup correspond to different structured water shells and degree of hydration inside and outside the SUV, with both effects being more pronounced for the outer CH_2-ethyl group. This could explain, at least in part, why chaotropic anions (by disrupting the hydration shell) affect mainly the outer $^{13}CH_2$-ethyl resonance, shifting it downfield.

The splitting of the carbonyl signal of PEth in SUVs into the inner and outer components also reflects the differences in packing conditions in two monolayers, as was previously observed for PC [16,24]. Earlier [24], it was suggested that those structural differences in phospholipid packing result in higher hydration of the carbonyl moiety (the C = O group hydrogen bond formation) in the outer loosely packed leaflet which, in turn, causes a downfield shift of the outer $^{13}C = O$ resonance. This high sensitivity of the carbonyl signal chemical shift to the hydrophobicity of the environment was previously used to characterize the localization of acyl neutral lipids, i.e., di- and triacylglycerols and cholesteryl esters, in serum lipoprotein particles (either outside on the surface or inside in the hydrophobic core), membranes and model mixtures (e.g., [30–32]). If indeed the carbonyl splitting in highly curved membranes reports different hydration on the outer and inner surfaces [24], we have to conclude that PEth molecules in the SUV are less hydrated in both leaflets than other naturally occurring phospholipids, whether zwitterionic or negatively charged (i.e., PC or PG). Moreover, like all phospholipids in the SUVs, the outer PEth molecules are more hydrated than the inner ones.

The reduced hydration of PEth compared to other phospholipids, attributed solely to its relatively hydrophobic headgroup, might have an unusual consequence. PEth may be embedded more deeply than PC in the bilayer which, in turn, could create local defects in the phospholipid packing. Moreover, the high sensitivity of the ^{13}C-carbonyl signals to the transleaflet difference in packing constraints, characteristic for all phospholipids, probably stems from the location of their C = O groups at a level inside the bilayer where this difference is particularly pronounced. The unusual upfield shift of the C_3-glycerol peak of PEth also favors this suggestion. If this interpretation is correct, the PEth position deeper into the lipid interior could bring some of its headgroup segments closer to that packing-sensitive area, as a result of which some ^{13}C-resonances from those groups become split into inner and outer components. Such an unusual conformation/orientation of PEth combined with its reduced hydration may also help explain why PEth can promote the formation of non-bilayer structures in model phospholipid systems [29,33]; it was suggested earlier [34] that the smaller amount of water bound to the headgroup of PE could be responsible for the tendency of this phospholipid to form hexagonal H_{II} phase.

In conclusion, in this work we demonstrated that $^{13}CH_2$-ethyl labeled PEth can be used successfully to detect the transbilayer difference in lipid packing density in SUVs. This unique sensitivity of PEth to local lipid packing density may have wider applicability and there are no obvious obstacles to prevent this naturally occurring

lipid from being employed in larger aggregates, like LUVs or even biological membranes, to probe the presence of a packing constraints gradient across the bilayer.

Acknowledgements

This work was supported by US Public Health Service Grants AA07186, AA07215, AA08714.

References

[1] Op den Kamp, J. (1979) Annu. Rev. Biochem. 48, 47–71.
[2] Devaux, P.F. (1991) Biochemistry 30, 1163–1173.
[3] Kroon, P.A., Kainosho, M. and Chan, S.I. (1976) Biochim. Biophys. Acta 433, 282–293.
[4] Eisenberg, K.E. and Chan, S.I. (1980) Biochim. Biophys. Acta 599, 330–335.
[5] Brouillette, C.G., Segrest, J.P., Ng, T.C. and Jones, J.L. (1982) Biochemistry 21, 4569–4575.
[6] Schuh, J.R., Banerjee, U., Muller, L. and Chan, S.I. (1982) Biochim. Biophys. Acta 687, 219–225.
[7] Jendrasiak, G.L., Smith, R. and Ribeiro, A.A. (1993) Biochim. Biophys. Acta 1145, 25–32.
[8] Victorov, A.V., Janes, N., Moehren, G., Rubin, E., Taraschi, T.F. and Hoek, J.B. (1994) J. Am. Chem. Soc. 116, 4050–4052.
[9] Alling, C., Gustavsson, L., Mansson, J.-E., Benthin, G. and Anggard, E. (1984) Biochim. Biophys. Acta 793, 119–122.
[10] Moehren, G., Gustavsson, L. and Hoek, J.B. (1994) J. Biol. Chem. 269, 838–848.
[11] Gustavsson, L. (1995) Alcohol Alcoholism 30, 391–406.
[12] Browning, J.L. (1981) Biochemistry 20, 7123–7133.
[13] Omodeo-Sale, F., Cestaro, B., Mascherpa, A., Monti, D. and Masserini, M. (1989) Chem. Phys. Lipids 50, 135–142.
[14] Klein, R.A. (1970) Biochim. Biophys. Acta 210, 485–489.
[15] Barsukov, L.I., Victorov, A.V., Vasilenko, I.A., Evstigneeva, R.P. and Bergelson, L.D. (1980) Biochim. Biophys. Acta 598, 153–168.
[16] Shapiro, Yu.E., Viktorov, A.V., Volkova, V.I., Barsukov, L.I., Bystrov, V.F. and Bergelson, L.D. (1975) Chem. Phys. Lipids 14, 227–232.
[17] Hong, M., Schmidt-Rorh, K. and Nanz, D. (1995) Biophys. J. 69, 1939–1950.
[18] Sundberg, S.A. and Hubbell, W.L. (1986) Biophys. J. 49, 553–562.
[19] McIntosh, T.J., Magid, A.D. and Simon, A. (1989) Biochemistry 28, 7904–7912.
[20] Fenske D.B. and Cullis, P.R. (1993) Biophys. J. 64, 1482–1491.
[21] Marsh, D. (1990) CRC Handbook of Lipid Bilayers, p. 82, CRC Press, Boca Raton.
[22] Barsukov, L.I., Volkova, V.I., Viktorov, A.V., Shapiro, Yu.E., Bystrov, V.F. and Bergelson, L.D. (1977) Bioorg. Khim. 3, 1355–1361.
[23] Rydall, J.R. and Macdonald, P.M. (1992) Biochemistry 31, 1092–1099.
[24] Schmidt, C.F., Barenholz, Y. and Thompson, T.E. (1977) Biochemistry 16, 3948–3953.
[25] Hutton, W.C., Yeagle, P.L. and Martin, R.B. (1977) Chem. Phys. Lipids 19, 255–265.
[26] Trauble, H. (1977) Membrane electrostatics, in Structure and Function of Biological Membranes, pp. 509–550, Plenum Press, New York.
[27] Hauser, H., Pascher, I., Pearson, R.H. and Sundell, S. (1981) Biochim. Biophys. Acta 650, 21–51.
[28] Nagle, J.F. (1993) Biophys. J. 64, 1476–1481.
[29] Lee, Y.-C., Zheng, Y.O., Taraschi, T.F. and Janes, N. (1996) Biochemistry, in press.
[30] Hamilton, J.A. and Small, D.M. (1981) Proc. Natl. Acad. Sci. USA 78, 6878–6882.
[31] Hamilton, J.A., Bhamidipati, S.P., Kodali, D.R. and Small, D.M. (1991) J. Biol. Chem. 266, 1177–1186.
[32] Hamilton, J.A., Cordes, E.H. and Glueck, C.J. (1979) J. Biol. Chem. 254, 5435–5441.
[33] Lee, Y.-C., Taraschi, T.F. and Janes, N. (1993) Biophys. J. 65, 1429–1432.
[34] Yeagle, P.L. and Sen, A. (1986) Biochemistry 25, 7518–7522.